ASTM INTERNATIONAL

Geotechnical Testing Journal

Seyed Mustapha Rahmaninezhad,[1] Jie Han,[2] Jamal Ismael Kakrasul,[1,3] and Mehari Weldu[4]

DOI: 10.1520/GTJ20180102

Stress Distributions and Pullout Responses of Extensible and Inextensible Reinforcement in Soil Using Different Normal Loading Methods

Geotechnical Testing Journal

doi:10.1520/GTJ20180102 available online at www.astm.org

Seyed Mustapha Rahmaninezhad,[1] Jie Han,[2] Jamal Ismael Kakrasul,[1,3] and Mehari Weldu[4]

Stress Distributions and Pullout Responses of Extensible and Inextensible Reinforcement in Soil Using Different Normal Loading Methods

Reference

Rahmaninezhad, S. M., Han, J., Kakrasul, J. I., and Weldu, M., "Stress Distributions and Pullout Responses of Extensible and Inextensible Reinforcement in Soil Using Different Normal Loading Methods," *Geotechnical Testing Journal* https://doi.org/10.1520/GTJ20180102. ISSN 0149-6115

ABSTRACT

In design of reinforced soil structures, pullout capacity of reinforcement in an anchorage zone is an important parameter for stability analysis. This parameter is generally quantified by conducting laboratory or field pullout tests. In the laboratory pullout test, the reinforcement is embedded in the soil mass at a normal stress, which is commonly applied by a pressurized airbag or a hydraulic jack through a rigid plate, and then a horizontal tensile force is applied to the reinforcement. This article reports an experimental study conducted to evaluate the effect of the load application method using an airbag with and without stiff wooden plates on the vertical stress distribution and the pullout capacities and deformations of extensible (geogrid) and inextensible reinforcement (steel strip) in the soil in a large pullout box. This study monitored the distributions of the vertical earth pressures at the top and bottom of the soil mass in the pullout box, and at the level of reinforcement using earth pressure cells. The measured earth pressures show that the airbag with stiff plates resulted in a nonuniform pressure distribution, whereas the tests with an airbag directly on the soil had an approximately uniform pressure distribution. The nonuniform pressure distribution resulting from the airbag with stiff plates reduced the pullout resistance of the reinforcement as compared with that using the same airbag without stiff plates. The nonuniform pressure distribution effect was more significant for narrow

Manuscript received March 31, 2018; accepted for publication September 17, 2018; published online November 5, 2018.

[1] Department of Civil, Environmental, and Architectural Engineering, The University of Kansas, 1530 W. 15th St., Lawrence, KS 66045, USA

[2] Department of Civil, Environmental, and Architectural Engineering, The University of Kansas, 2150 Learned Hall, 1530 W. 15th St., Lawrence, KS 66045, USA (Corresponding author), e-mail: jiehan@ku.edu, https://orcid.org/0000-0003-3137-733X

[3] Department of Civil Engineering, Soran University, Kawa St., Soran 44008, Iraq

[4] Maccaferri Inc., 9210 Corporate Blvd., No. 220, Rockville, MD 20850, USA

inextensible reinforcements than wide extensile reinforcements. The test results also show that the displacements in the cross section of the same transverse bar were not equal when the normal load was applied through stiff plates.

Keywords

displacement, geogrid, normal stress, pullout, steel strip

Introduction

In reinforced walls and slopes, failure may happen along a potential failure plane if it is not well designed (Han and Leshchinsky 2006; Berg, Christopher, and Samtani 2009; Patra and Shahu 2012; and Han 2015). This failure plane divides the wall or slope into two zones: unstable and stable zones. The reinforcement may rupture or be pulled out from soil at the front or rear as illustrated in Han (2015). Mobilization of tension in the reinforcement near the potential failure plane is important for possible pullout failure of the reinforcement (Ochiai et al. 1996; Sieira, Gerscovich, and Sayão 2009; Patra and Shahu 2012). The pullout failure of the reinforcement is considered one of the controlling mechanisms for internal instability of reinforced walls and slopes (Jayawickrama et al. 2014). Internal stability analysis due to pullout failure is mainly aimed at assessing pullout resistance versus maximum tension in the reinforcement. The pullout resistance depends on length, geometry, and surface roughness of reinforcement, soil properties, normal stress, and integrity of facing elements. In the past, experimental pullout tests and numerical studies have been carried out to investigate the soil-reinforcement interaction mechanisms and their influence factors (e.g., Madhav, Gurung, and Iwao, 1998; Palmeira 2004; Huang and Bathurst 2009; Sieira, Gerscovich, and Sayão 2009; Palmeira 2009; Ezzein and Bathurst 2014; Sukmak et al. 2015; Weldu et al. 2015; Wang, Jacobs, and Ziegler 2016; Weldu et al. 2016; Zornberg, Roodi, and Gupta 2017; Roodi and Zornberg 2017).

The pullout test procedure includes preparation of the test specimen, application of the normal pressure, and application of the pullout force (Jayawickrama et al. 2014). ASTM D6706-01, *Standard Test Method for Measuring Geosynthetic Pullout Resistance in Soil*, standardized the test method using pullout box equipment. A typical pullout box is an open rigid box consisting of two smooth parallel sides, a back wall, a horizontal split removable cap, a bottom plate, and a load transfer sleeve. The literature review on pullout testing of extensible reinforcement (geogrids) and inextensible reinforcement (steel strips) shows several limitations of the current pullout box equipment (e.g., Palmeira 2009). One of the limitations is that the reinforcement and soil are not visible and so the pullout load acting throughout the reinforcement can only be recorded at the test apparatus boundaries, mostly at the front end of the specimen (Bathurst and Ezzein 2015). The relative soil-reinforcement movement that occurs on the plane of the reinforcement cannot be determined quantitatively (Ezzein and Bathurst 2014). To overcome this limitation, researchers have used strain gages or displacement transducers attached to the reinforcement (especially for geogrids) at different locations within the soil to find out their corresponding local or global strains (e.g., Sieira, Gerscovich, and Sayão 2009; Jayawickrama et al. 2014; Rahmaninezhad et al. 2016). Also, in some studies, X-ray radiography or computed tomography scanners have been used to show the soil movement in small specimens of reinforced soil (Otani et al. 2001; Sugimoto, Alagiyawanna, and Kadoguchi 2001).

Another major issue with current pullout boxes is related to how a normal stress is applied. Commonly, a normal stress is applied to the reinforced soil in the pullout box to simulate the overburden pressure in the field. Therefore, the normal stress must be uniform and constant during the pullout test. ASTM D6706-01 recommends a flexible pneumatic or hydraulic diaphragm-loading device, which covers the whole area of the pullout box to maintain a uniform normal stress. In many studies, an airbag was used to apply normal stresses to the reinforced soil mass (e.g., Palmeira 2004; Teixeira, Bueno, and Zornberg 2007; Nayeri and Fakharian 2009; Ezzein and Bathurst 2014; Weldu et al. 2016). To protect the airbag from damage by aggregates, plates (e.g., steel plates or wooden plates) are placed under the airbag (e.g., Lajevardi, Dias, and Racinais 2013; Lawson et al. 2013). In some cases, however, a hydraulic jack was used to apply the normal stress through a rigid plate (Abdelrahman, Ashmawy, and Abdelmoniem 2008; Abdi and Arjomand 2011). However, Leshchinsky and Marcozzi (1990) pointed out that the stiffness of the foundations and the type of the soil have effects on the distribution of the contact pressure. Therefore, it is important to evaluate the possible effect of plates under the airbag on the measured pullout capacity of reinforcement in soil. Rahmaninezhad et al. (2016) conducted a preliminary study illustrating the possible effect of the plates on the pullout capacity of the reinforcement. In this article, an in-depth study was conducted to examine the stress distributions at different normal loads applied by a flexible airbag with and without stiff plates. These distributions were measured at three levels of the soil mass (at the top of the compacted reinforced soil, the level of the reinforcement, and the bottom of the pullout box). In addition, the effects of these methods of applying normal stresses on the pullout resistance of the extensible reinforcement (uniaxial geogrid) and the inextensible reinforcement (steel strip) as well as the deformation of the reinforcement were investigated.

Test Device and Materials

PULLOUT BOX

In this study, a pullout box was designed and fabricated in the Geotechnical Laboratory at the University of Kansas in accordance with ASTM D6706-01 recommendations. The box was made of steel and has inner dimensions measuring 1.5 m long, 0.6 m wide, and 0.6 m high, which exceeds the minimum dimensions recommended by ASTM D6706-01. The pullout box has a 0.045-m-high by 0.5-m-long slot on the front wall. To minimize the arching effect during pullout tests, a 0.15-m-wide sleeve was fixed on the inner side of the front wall, right above the slot. Also, the sleeve may reduce the influence of the box front face (Palmeira 2009). **Fig. 1** shows the pullout box after the fabrication.

MATERIALS

The laboratory pullout tests were carried out on extensible reinforcement (punched-drawn uniaxial polypropylene (PP) geogrid modified from a biaxial geogrid) embedded in Kansas River sand and inextensible reinforcement (ribbed steel strip) in crushed limestone aggregate. Particle size distribution tests were conducted using ASTM D422, *Standard Test Method for Particle-Size Analysis of Soils*. A standard direct shear test was used to determine the friction angle for the sand compacted at 70 % relative density. That test was conducted according to ASTM D3080, *Standard Test Method for Direct Shear Test of Soils under Consolidated Drained Conditions.* However, the friction angle for the aggregate was determined using triaxial compression tests according to ASTM D7181, *Standard Test Method for Consolidated Drained Triaxial Compression Test for Soils*. The minimum and

FIG. 1

Pullout box.

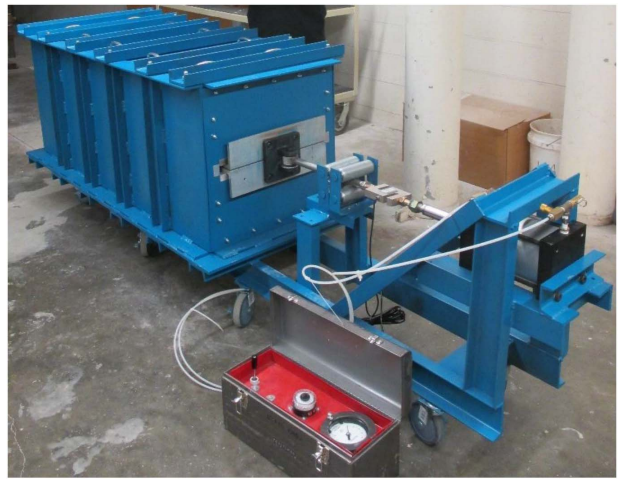

maximum dry densities for both backfill materials were obtained by the index density methods according to ASTM D4254, *Standard Test Methods for Minimum Index Density and Unit Weight of Soils and Calculation of Relative Density*, and ASTM D4253, *Standard Test Methods for Maximum Index Density and Unit Weight of Soils Using a Vibratory Table*, respectively. Table 1 summarizes the physical properties, the Unified Soil Classification System classification, and the angle of friction of the backfill materials used in the pullout tests.

A uniaxial geogrid modified from a punched-drawn biaxial PP geogrid, as an extensible reinforcement, was used in this experimental study. This geogrid was selected because it has been adopted in our model tests and its in-air load-strain properties were determined by a previous study (Xiao, Han, and Zhang 2016). Considering the fact that uniaxial geogrid is commonly used in reinforced walls or slopes, three transverse ribs (i.e., the cross-machine direction ribs) of the biaxial geogrid were removed in every four ribs to create a shape of uniaxial geogrid. Xiao, Han, and Zhang (2016) first adopted this modification, and then Rahmaninezhad et al. (2016) and Kakrasul et al. (2016) used it in their model studies. The longitudinal ribs (i.e., the machine direction ribs) and the transverse members of the geogrid contribute to the total pullout resistance. In other words, the total pullout resistance is the sum of the frictional resistance on the geogrid surface and the bearing

TABLE 1

Properties of backfill materials.

Property	Kansas River Sand	Crushed Aggregate
Coefficient of uniformity, C_u	3.18	14
Coefficient of curvature, C_c	0.93	2.57
USCS classification	SP	GW
Mean particle size, D_{50}, mm	0.56	10
Minimum dry unit weight, kN/m^3	16.0	14.9
Maximum dry unit weight, kN/m^3	18.8	18.6
Angle of friction, °	37	46

Note: USCS = Unified Soil Classification System.

TABLE 2
Properties of the biaxial geogrid (provided by the manufacturer).

Index Properties	MD	XMD
Aperture dimensions, mm	25	33
Minimum rib thickness, mm	0.76	0.76
Tensile strength at 2 % strain, kN/m	4.1	6.6
Tensile strength at 5 % strain, kN/m	8.5	13.4
Ultimate tensile strength, kN/m	12.4	19

Note: MD = machine direction; XMD = cross-machine direction.

resistance of the transverse members (Tran, Meguid, and Chouinard 2013). Alagiyawanna et al. (2001) found that removal of 75 % of the transverse ribs reduced the reinforcing effect of the geogrid on the sand movement. **Table 2** provides the properties of the biaxial geogrid. In this study, one uniaxial geogrid that was 300 mm wide and 600 mm long was used in the evaluation of vertical pressure distribution while another uniaxial geogrid specimen that was 370 mm wide and 765 mm long was used in the evaluation of pullout behavior. These geogrid samples before the removal of transverse ribs had an ultimate tensile strength of 12.4 kN/m in the machine direction and 19 kN/m in the cross-machine direction.

A galvanized ribbed steel strip as inextensible reinforcement was used in this study. This strip reinforcement was 1,500 mm long, 50 mm wide, and 4 mm thick. It had 3-mm-high ribs on both the top and bottom faces to increase pullout resistance. The effective embedment length of the steel strip in the pullout box was 1.2 m.

INSTRUMENTATION

The instrumentation included a load cell, displacement transducers, pressure cells, a pressure gauge, and a data acquisition system. An S-shaped load cell with a capacity of 50 kN was used to measure the pullout force. Five displacement transducers were used to measure the displacements at the junctions of the geogrid. These transducers were connected to the geogrid by steel rods that were extended from junctions out to the rear side of the box. Similarly, two displacement transducers were used to measure the displacements at the front and rear ends of the strip reinforcement. Strain gauge–type earth pressure cells 25 mm in diameter were installed to evaluate the normal stresses at different levels of the soil mass. The capacities of these earth pressure cells were 200 and 500 kPa, respectively. A pressure gauge was used to control the pressure applied to the airbag.

Test Procedure

The procedure for preparing a pullout test included filling half of the box with the backfill material and compaction, placement of the reinforcement, installation of sensors and connection to the data acquisition system, and continuous filling of the box with the remaining backfill. The backfill material was placed into the box in two layers, and each layer was compacted until the minimum relative density of 70 % was achieved. The effect of compaction on the reinforced sand for reduced-scale models was discussed in Rahmaninezhad, Yasrobi, and Eftekharzadeh (2009). The geogrid or steel strip was embedded in the middle of the backfill height (i.e., at the same elevation of the clamp), and attached to the pullout load assembly. Because the connection between the hydraulic jack and the clamp was relatively rigid, the pullout force was applied horizontally. Moreover, the clamp was placed

FIG. 2

Schematic view of the cross sections of the pullout box with (a) the airbag on the soil and (b) the airbag on the stiff wood plates.

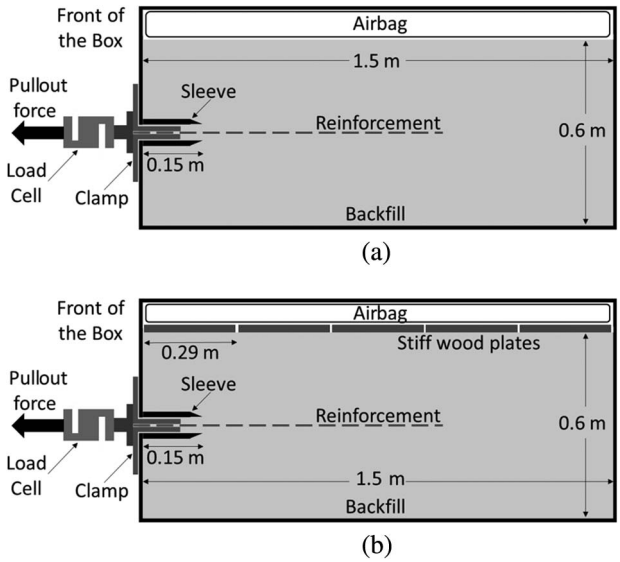

between the sleeves, which prevented the rotation of the clamp. Finally, all the sensors, including the displacement transducers, the earth pressure cells, the load cell, and the pressure gauge, were installed at their desired locations. Normal stress was applied with a pressurized airbag placed on the top of the compacted backfill. This airbag allowed soil dilation or contraction during pullout testing and maintained a constant normal stress. To simulate the reinforcement at different elevations of a wall in the field, three normal stresses were selected for each reinforcement type. In some tests, five wood plates that were 0.58 m long, 0.29 m wide, and 0.05 m thick were placed on top of the compacted backfill, one next to another, before the placement of the airbag. Once the whole pullout test setup was completed, all sensors were activated to allow the data acquisition system to start recording. After the normal stress distribution throughout the soil mass became stable, the pullout load was applied using a double-acting hydraulic jack. Fig. 2 shows the schematic view of the cross sections of the pullout box, in which one did not have stiff wood plates and the other did.

Test Results

DISTRIBUTION OF NORMAL STRESS

In this study, 21 earth pressure cells were used to examine the distributions of the vertical pressures at the top and the bottom of the soil mass and at the level of the reinforcement in the pullout box. Fig. 3 illustrates the arrangement of the earth pressure cells on the top of the reinforced soil mass. The variations of the measured vertical pressures under different normal stresses across the box width (axis A-A) and the box length (axis B-B) are shown in Figs. 4 and 5, respectively. The measured vertical pressures presented in these figures are the additional vertical stresses induced by the applied normal pressures. In these two figures, it was assumed that the distributions of the vertical pressures across the box width (i.e., the transversal section) were symmetric. Fig. 4a shows that when the airbag was used without stiff plates, the vertical pressure concentrated in the middle of the box. On the

FIG. 3

The arrangement of the earth pressure cells on top of the soil mass.

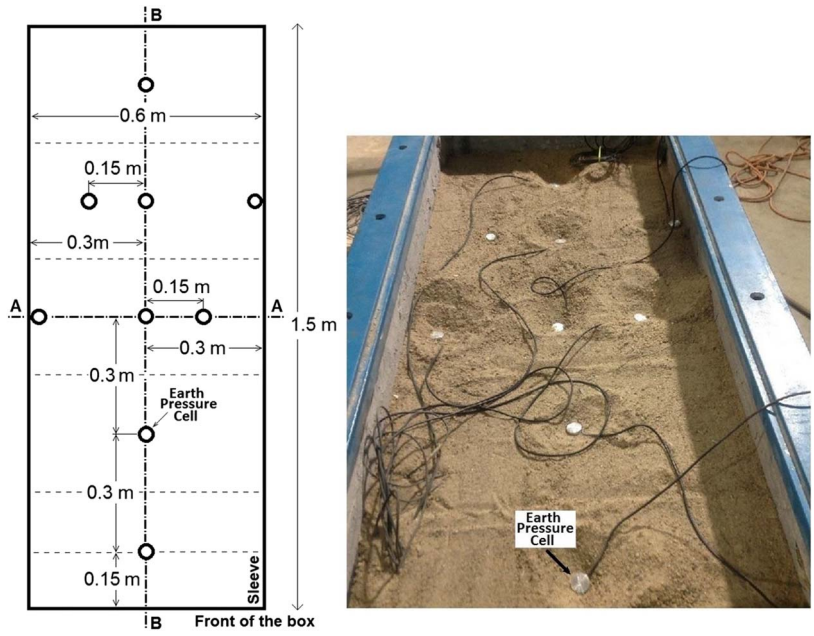

FIG. 4 Variations of the measured vertical pressures on top of the soil and across the box width (axis A-A) under different normal stresses applied by (a) the airbag without stiff plates and (b) the airbag with stiff plates.

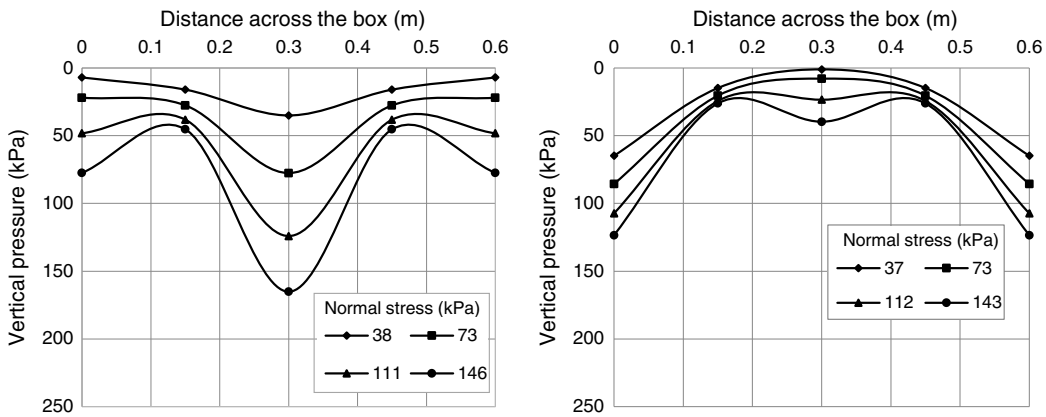

(a) (b)

other hand, when the normal stress was applied by the airbag with stiff plates, the maximum measured vertical pressures were close to the sides of the box (Fig. 4b). Likewise, on the longitudinal section of the box (i.e., the axis B-B), when the airbag was used without any stiff plates, the measured maximum vertical pressures were higher than those using the stiff plates as shown in Fig. 5a and b. However, Figs. 4 and 5 imply that the application of the normal load by the airbag without any stiff plates (as a flexible diaphragm) resulted in a more uniform pressure distribution than that by the airbag with stiff plates.

FIG. 5 Variations of the measured vertical pressures on top of the soil and across the box length (axis B-B) under the normal stresses applied by (a) the airbag without stiff plates and (b) the airbag with stiff plates.

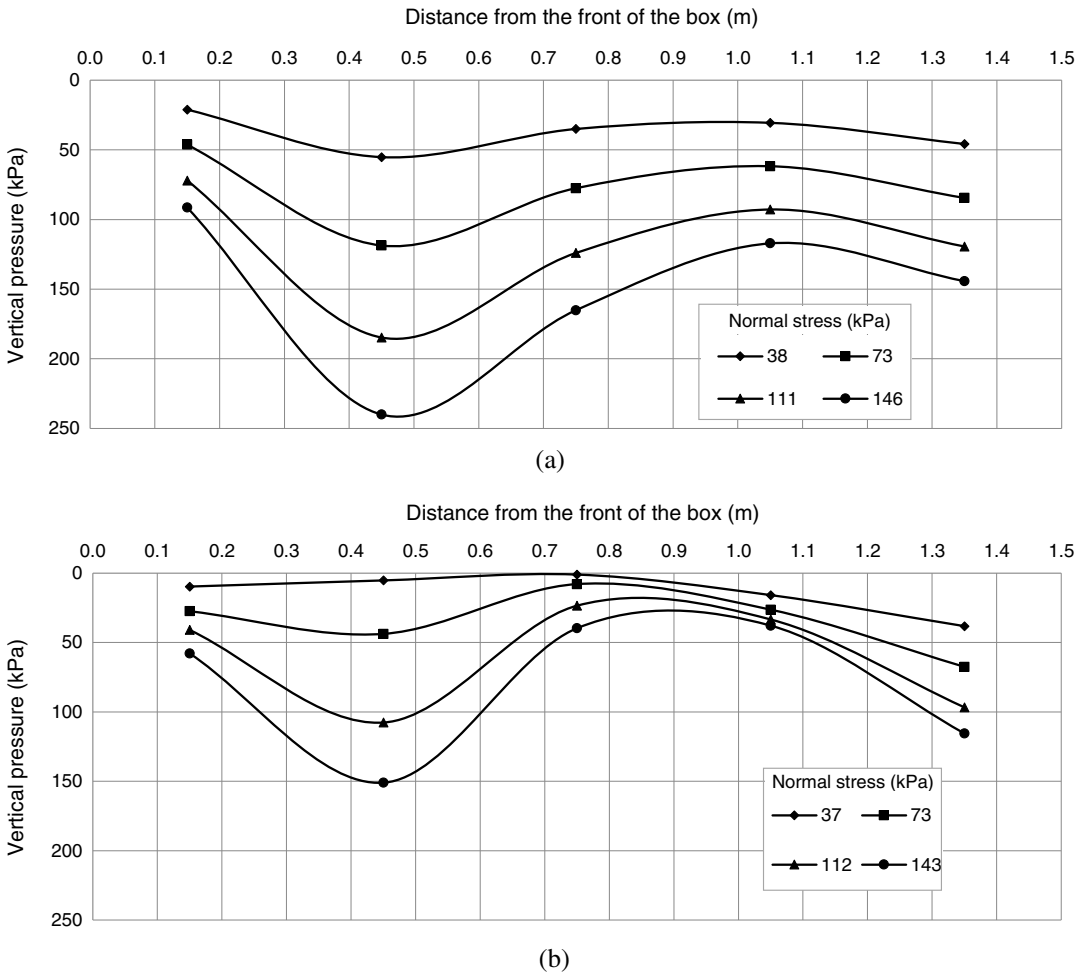

Sugimoto, Alagiyawanna, and Kadoguchi (2001) and Palmeira (2009) found that the conditions of the frontal face of the pullout box might have a noticeable effect on the pullout behavior of the reinforcement. Researchers suggested using a lubricated frontal or movable/flexible frontal face, or both, with a sleeve, to keep the reinforcement distant from the front wall of the pullout box (e.g., Wilson-Fahmy, Koerner, and Sansone 1994; Perkins and Cuelho 1999; Sugimoto, Alagiyawanna, and Kadoguchi 2001; Palmeira 2009). Palmeira (2009) found that the use of a sleeve yielded the maximum pullout resistance that was higher than that observed in the case of using a lubricated frontal face. It appears that the sleeve had less influence on the pullout test result than the box frontal wall; however, the sleeve still changed the uniformity of the distribution of the vertical pressure near the front of the box as shown in **Fig. 5a**. The result indicates that the measured vertical pressure behind the sleeve was consistently lower than the applied normal stress. This finding is consistent with that by Bathurst et al. (2001) on the vertical load transfer from the soil to the rigid sleeve.

FIG. 6

The layout of the earth pressure cells on the bottom of the soil mass.

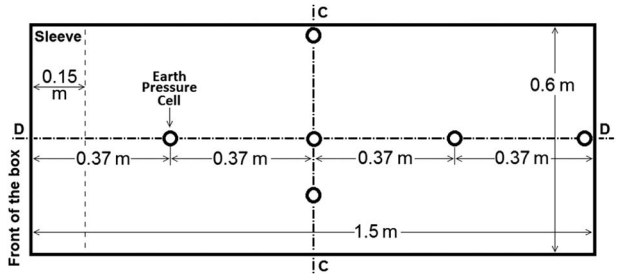

FIG. 7 Variations of the measured vertical pressures on the bottom of the box under different normal stresses applied by the airbag without any stiff plates along (a) the axis C-C and (b) the axis D-D.

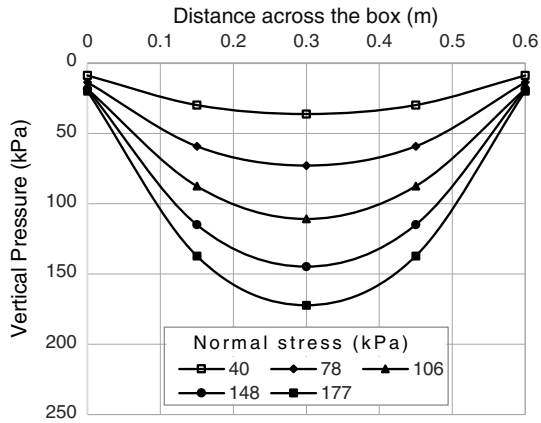

(a)

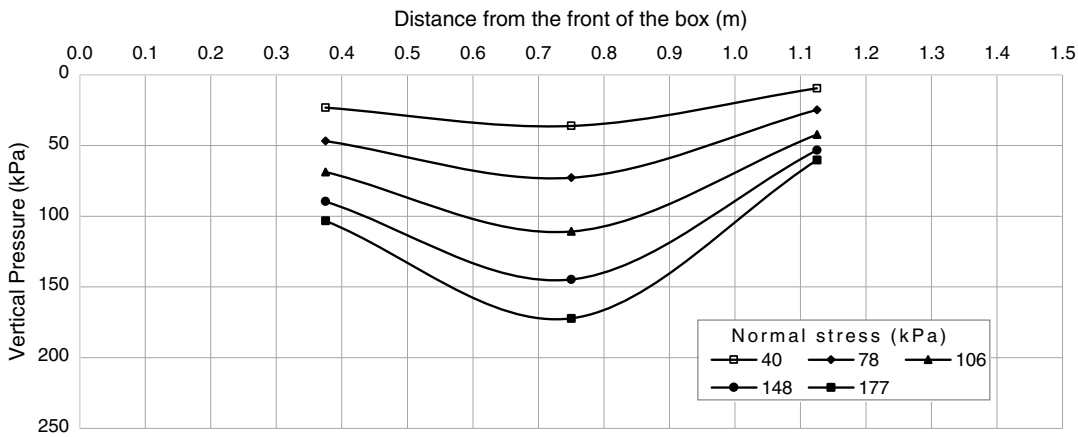

(b)

Fig. 6 shows the layout of the earth pressure cells on the bottom of the box. Fig. 7a and b shows the variations of the measured vertical pressures along the box width (i.e., the axis C-C) and length (i.e., the axis D-D), respectively, under different normal stresses applied by the airbag without any stiff plates. The maximum measured normal pressures on the bottom of the box happened in the center of the transverse section of the box. In the longitudinal section, the maximum vertical pressures were also in the center (Fig. 7b). On the top of the soil mass, however, the maximum vertical pressures happened near the front of the box (Fig. 5a).

Fig. 8 shows the layout of the earth pressure cells and the telltales on the level of the geogrid that was 300 mm wide and 600 mm long. The earth pressure cells were placed to determine the distribution of vertical pressures, while the telltales were fixed on the junctions of the geogrid following ASTM D6706-01 to determine the displacements of the geogrid along its length. The detail of the telltale measurements will be discussed later in this article. Fig. 9a shows the variations of the vertical pressures along the F-F section under different normal stresses applied by the airbag without any stiff plates. The

FIG. 8 Layout of the geogrid, the earth pressure cells, and the telltales.

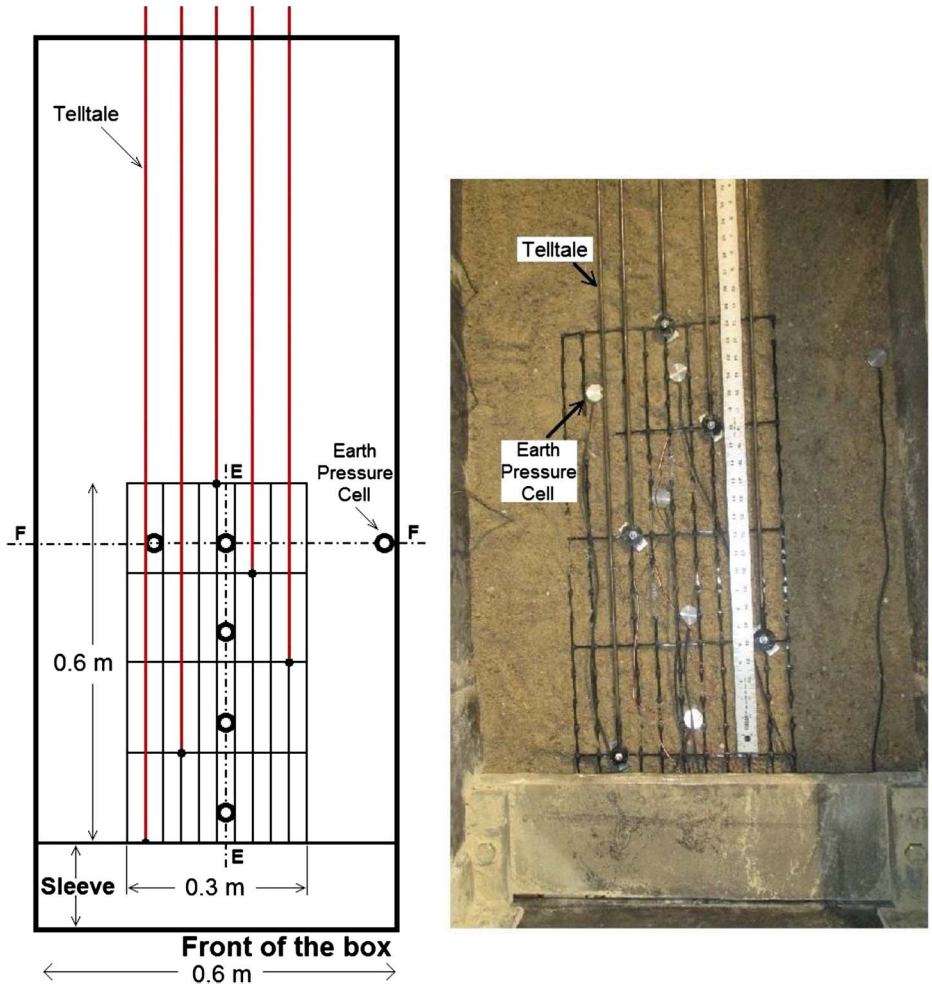

FIG. 9 Variations of the measured vertical pressures along the geogrid under different normal stresses applied by the airbag without any stiff plates along: (a) the axis F-F and (b) the axis E-E.

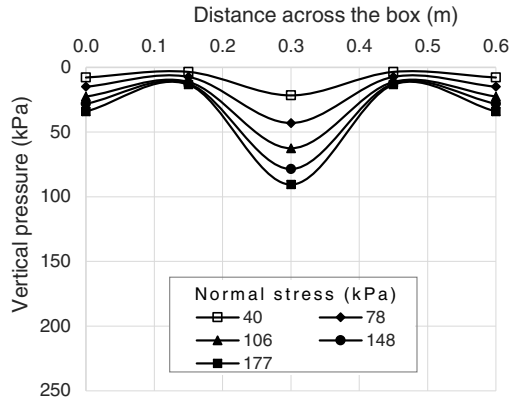

(a)

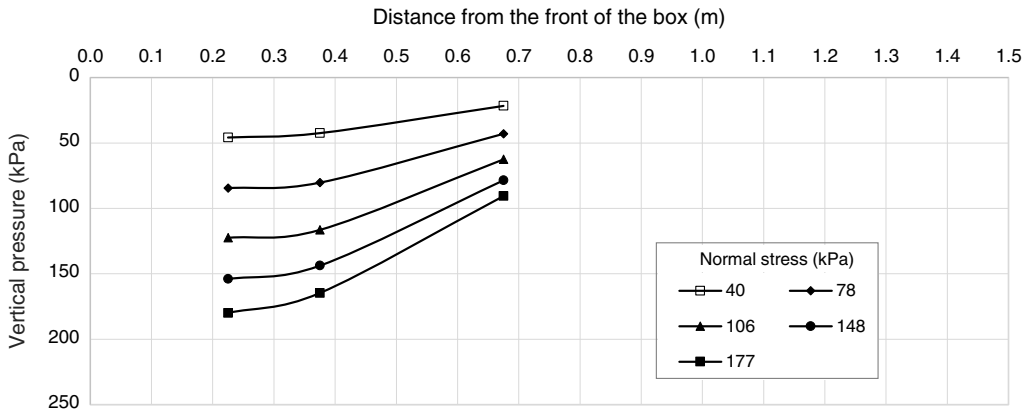

(b)

concentration of the vertical pressures was on the center of the transverse section of the box, on the level of the reinforcement. Fig. 9b displays the variations of the measured vertical pressures along the E-E section under different normal stresses applied by the airbag without any stiff plates. These distributions were measured just along the length of the geogrid. In some research (e.g., Jayawickrama et al. 2014; Wang, Jacobs, and Ziegler 2016), one or two earth pressure cells were placed along the central line of the pullout box under the airbag or stiff plates. Based on this study, the distribution of the vertical pressures along the centerline may not reflect the actual distribution of the vertical pressures.

PULLOUT RESISTANCE OF REINFORCEMENT

Pullout tests were carried out in this study to evaluate the effects of two different methods of applying the normal stress on the pullout resistance of the uniaxial geogrid and the ribbed steel strip embedded in the soil. In the geogrid tests, 370-mm-wide and 765-mm-long geogrids were used. Fig. 10 presents the pullout test results of the geogrids with two different

FIG. 10 Pullout force versus displacement of the geogrid under normal stresses applied by (a) the airbag without stiff plates and (b) the airbag with stiff plates.

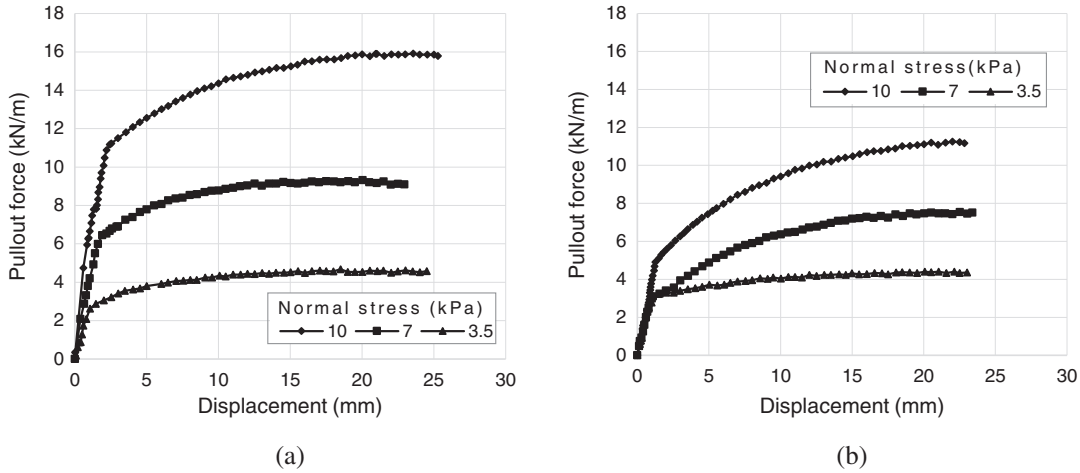

methods of applying the normal stress. These figures show that at the normal stress of 10 kPa applied by the airbag without and with stiff plates, the pullout forces were 15.87 and 11.11 kN/m, respectively, at the front displacement of 20 mm. Also, at the normal stress of 7 kPa applied by the airbag without and with stiff plates, the pullout forces were 9.32 and 7.47 kN/m, respectively, at the same front displacement (20 mm). Therefore, the pullout resistance of the geogrid under the airbag without any stiff plates was higher than that under the airbag with stiff plates. Under the normal stresses of 10, 7, and 3.5 kPa, the pullout resistance values of the geogrid when the airbag was used with stiff plates were 30, 20, and 3 %, respectively, lower than those measured without stiff plates. Evidently, at the low normal stress, there was a minor difference between the pullout resistances using these two different loading methods.

Fig. 11 shows that the strip reinforcement was embedded in the middle of the gravel and attached to the pullout load assembly. Fig. 12 shows the results of the pullout

FIG. 11

Ribbed steel strip placed in the box.

FIG. 12 Pullout force versus displacement of the ribbed steel strip under different normal stresses applied by (a) the airbag without stiff plates and (b) the airbag with stiff plates.

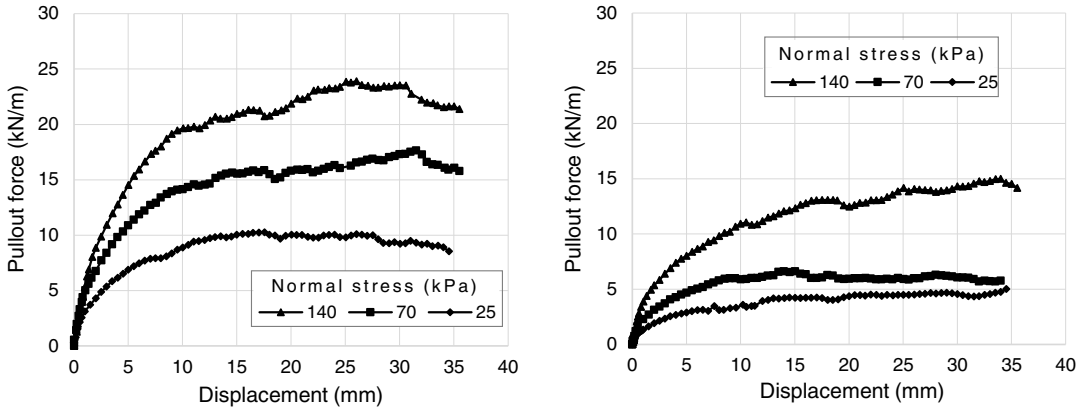

resistance of the ribbed steel strip reinforcement. The pullout resistance when the normal stress was applied by the airbag without stiff plates was higher than that with stiff plates. Under the normal pressures of 140, 70, and 25 kPa, the pullout resistance values when the airbag was used with stiff plates were 45, 62, and 65 % lower than those without stiff plates, respectively. As discussed earlier, in the center of the box there was the concentration of the normal stress applied by the airbag without stiff plates, while there was the reduction of the normal stress by the airbag with stiff plate. The pullout resistance of the steel strip was higher when no stiff plate was used than when stiff plates were used. When these results are compared to those of the geogrid, it can be concluded that these loading methods had a more significant effect on the pullout resistance of the narrow reinforcement (i.e., the steel strip) than the wide reinforcement (i.e., the geogrid).

DISPLACEMENT AND STRAIN OF GEOGRID

To investigate the effect of these two different methods of applying the normal stress on the deformation of the geogrid, two tests were conducted by attaching five telltale rods on the junctions of one transverse rib as shown in **Fig. 13**. **Fig. 14** shows the measured displacements at these junctions under different pullout forces when a normal stress of 10 kPa was applied using the airbag without and with stiff plates. **Fig. 14a** shows that the displacements of the geogrid at the junctions were nearly uniform because the airbag without stiff plates generated the nearly uniform distribution of the vertical pressures in the center of the box as shown in **Figs. 14a** and **9a**.

Fig. 14b shows that when the stiff plates were used, the maximum displacement at the junctions of the geogrid occurred in the middle of the longitudinal ribs, and the minimum displacements at the junctions occurred near the sides of the box. This result can be explained based on the distribution of the vertical pressures in the transverse section of the box as shown in **Fig. 4b**, i.e., the lowest vertical pressure at the center and the highest vertical pressure at the edges of the box.

Fig. 14 shows that the measured displacements along the transverse bar of the geogrid were different. However, most researchers have placed the telltales on the junctions of

FIG. 13

Telltale rods attached on the junctions of the transverse rib.

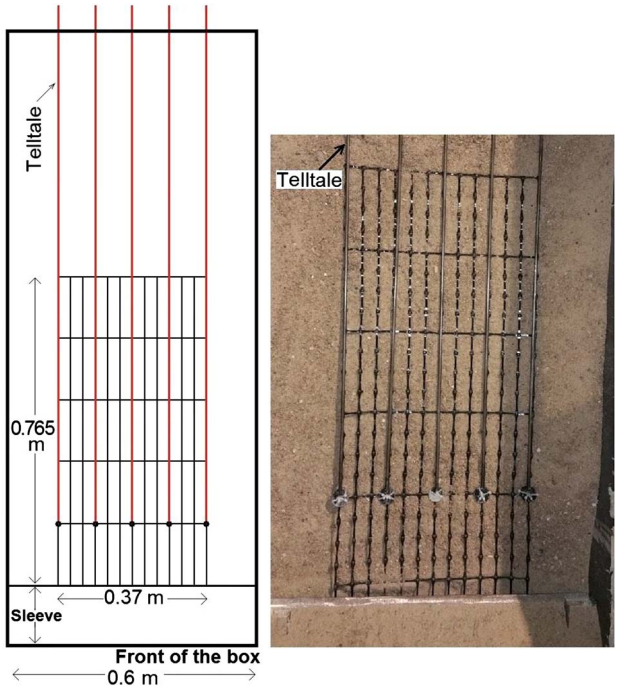

FIG. 14 Displacements of the junctions on the transverse rib under different applied pullout forces under the normal stress of 10 kPa by (a) the airbag without stiff plates and (b) the airbag with stiff plates.

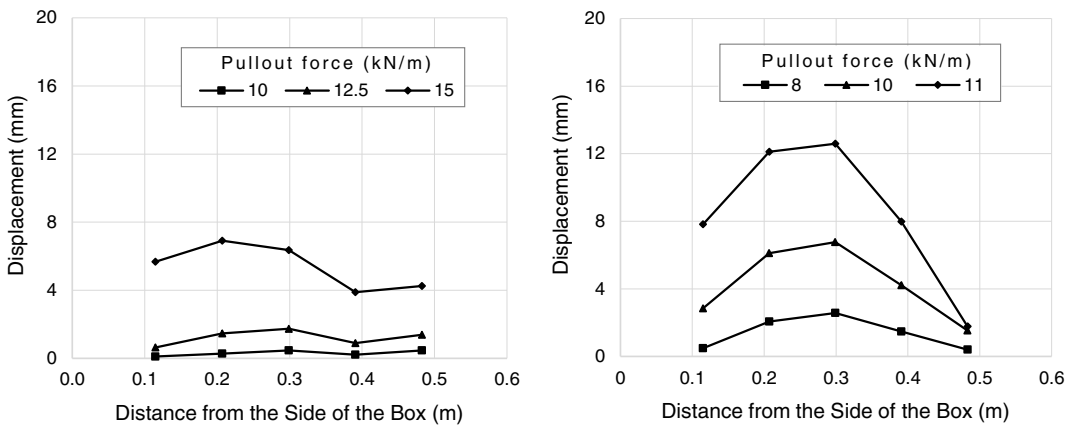

the geogrid along the longitudinal direction with an offset in the transverse direction (e.g., Nayeri and Fakharian 2009; Ferreira and Zornberg 2015; Wang, Jacobs, and Ziegler 2016). This arrangement of telltales may result in misleading displacement results that yield inaccurate calculations of tensile strains in the geogrid.

Conclusions

The objective of this study was to evaluate the effects of the stiff plates under the airbag on the distributions of the vertical stresses, the pullout capacities, and the displacements of the reinforcement in the pullout tests. To achieve this objective, several large-scale pullout tests were conducted, in which the geogrid and the ribbed steel strip were placed within the soil mass. The following conclusions and recommendations can be made based on this experimental study:

(1) When the normal stresses were applied by the airbag without stiff plates, the measured maximum vertical pressures in the transverse direction on top of the soil mass occurred in the middle of the pullout box. However, in the case of the airbag with stiff plates, the maximum vertical pressures in the transverse direction were measured near the edges of the box.
(2) When the normal stress was applied by the airbag without the stiff plates, the distribution of the vertical pressures along the centerline in the longitudinal direction on top of the soil mass was more uniform, and the measured maximum vertical pressure was higher than that which was measured by the airbag on the stiff plates. Although the sleeve minimized the effect of the box front face, it still changed the uniformity of the distribution of the vertical pressure in front of the box.
(3) The maximum vertical pressure on the bottom of the box under the normal stresses applied by the airbag without stiff plates occurred in the middle of the box.
(4) When the normal stress was applied by the airbag without any stiff plates, the maximum vertical pressures at the level of the reinforcement in the transverse and longitudinal sections were in the middle and close to the front of the box, respectively.
(5) Because of the difference in the distribution of the vertical pressures, the pullout resistance of the geogrid under the normal stresses applied by the airbag without stiff plates was higher than that by the airbag with stiff plates. With the increase of the normal stress, their difference in the pullout resistance increased.
(6) Because of the difference in the distribution of the vertical pressures and the narrow steel strip, the pullout resistance of the steel strip under the normal stresses applied by the airbag without stiff plates was much higher than that with stiff plates. The comparison also showed that the stiff plates under the airbag had a more significant effect on the pullout resistance for the narrow steel strips than that for the wide geogrid.
(7) When the normal stress was applied by the airbag without stiff plates, the displacements at the transverse bar of the geogrid were approximately uniform. When the stiff plates were used, however, the low vertical pressures in the central zone of the box led to the maximum displacement of the geogrid at that location.

ACKNOWLEDGMENTS

The Bonner Spring Quarry APAC-Kansas City, Inc., the Tensar International, and Reinforced Earth Company provided the aggregate material, the geogrid, and the steel strip, respectively, used in this study. The laboratory managers and technicians, David Woody, Matthew Maksimowicz, Kent Dye, and Erick Nicholson, in Department of Civil, Environmental, and Architectural Engineering (CEAE) at the University of Kansas (KU) provided their technical support during the fabrication of the new pullout box and the laboratory pullout testing. Furthermore, the former graduate students, Dr. Yan Jiang, Dr. Jun Guo, Ghaith Abdulrasool, and Dr. Fei Wang, from the KU CEAE Department provided their assistance in collecting the aggregate material from the quarry and performing laboratory tests.

References

Abdelrahman, A. H., Ashmawy, A. K., and Abdelmoniem, M., 2008, "An Apparatus for Direct Shear, Pullout, and Uniaxial Testing of Geogrids," *Geotech. Test. J.*, Vol. 31, No. 6, pp. 470–479, https://doi.org/10.1520/GTJ100761

Abdi, M. R. and Arjomand, M. A., 2011, "Pullout Tests Conducted on Clay Reinforced with Geogrid Encapsulated in Thin Layers of Sand," *Geotext. Geomembr.*, Vol. 29, No. 6, pp. 588–595, https://doi.org/10.1016/j.geotexmem.2011.04.004

Alagiyawanna, A. M. N., Sugimoto, M., Sato, S., and Toyota, H., 2001, "Influence of Longitudinal and Transverse Members on Geogrid Pullout Behavior during Deformation," *Geotext. Geomembr.*, Vol. 19, No. 8, pp. 483–507, https://doi.org/10.1016/S0266-1144(01)00020-6

ASTM D422-63, 2007, *Standard Test Method for Particle-Size Analysis of Soils*, ASTM International, West Conshohocken, PA, www.astm.org

ASTM D3080/D3080M, 2011, *Standard Test Method for Direct Shear Test of Soils under Consolidated Drained Conditions*, ASTM International, West Conshohocken, PA, www.astm.org

ASTM D4253, 2016, *Standard Test Methods for Maximum Index Density and Unit Weight of Soils Using a Vibratory Table*, ASTM International, West Conshohocken, PA, www.astm.org

ASTM D4254, 2016, *Standard Test Methods for Minimum Index Density and Unit Weight of Soils and Calculation of Relative Density*, ASTM International, West Conshohocken, PA, www.astm.org

ASTM D6706-01, 2013, *Standard Test Method for Measuring Geosynthetic Pullout Resistance in Soil*, ASTM International, West Conshohocken, PA, www.astm.org

ASTM D7181, 2011, *Standard Test Method for Consolidated Drained Triaxial Compression Test for Soils*, ASTM International, West Conshohocken, PA, www.astm.org

Bathurst, R. J. and Ezzein, F. M., 2015, "Geogrid and Soil Displacement Observations during Pullout Using a Transparent Granular Soil," *Geotech. Test. J.*, Vol. 38, No. 5, pp. 1–13, https://doi.org/10.1520/GTJ20140145

Bathurst, R. J., Walters, D. L., Hatami, K., and Allen, T. M., 2001, "Full-Scale Performance Testing and Numerical Modelling of Reinforced Soil Retaining Walls," presented at the *Fourth International Symposium on Earth Reinforcement*, Fukuoka, Japan, A.A. Balkema, Rotterdam, the Netherlands, pp. 777–799.

Berg, R., Christopher, B. R., and Samtani, N., 2009, "Design and Construction of Mechanically Stabilized Earth Walls and Reinforced Soil Slopes – Volume I," FHWA-NHI-10-024 and FHWA FHWA GEC 011 – Volume I, U. S. Department of Transportation, Federal Highway Administration, Washington, DC, 306p.

Ezzein, F. M. and Bathurst, R. J., 2014, "A New Approach to Evaluate Soil-Geosynthetic Interaction Using a Novel Pullout Test Apparatus and Transparent Granular Soil," *Geotext. Geomembr.*, Vol. 42, No. 3, pp. 246–255, https://doi.org/10.1016/j.geotexmem.2014.04.003

Ferreira, J. A. and Zornberg, J. G., 2015, "A Transparent Pullout Testing Device for 3D Evaluation of Soil-Geogrid Interaction," *Geotech. Test. J.*, Vol. 38, No. 5, pp. 686–707, https://doi.org/10.1520/GTJ20140198

Han, J., 2015, *Principles and Practice of Ground Improvement*, John Wiley & Sons, Hoboken, NJ, p. 432.

Han, J. and Leshchinsky, D., 2006, "General Analytical Framework for Design of Flexible Reinforced Earth Structures," *J. Geotech. Geoenviron. Eng.*, Vol. 132, No. 11, 1427–1435, https://doi.org/10.1061/(ASCE)1090-0241(2006)132:11(1427)

Huang, B. and Bathurst, R. J., 2009, "Evaluation of Soil-Geogrid Pullout Models Using a Statistical Approach," *Geotech. Test. J.*, Vol. 32, No. 6, pp. 489–504, https://doi.org/10.1520/GTJ102460

Jayawickrama, P. W., Lawson, W. D., Wood, T. A., and Surles, J. G., 2014, "Pullout Resistance Factors for Steel MSE Reinforcements Embedded in Gravelly Backfill," *J. Geotech. Geoenviron. Eng.*, Vol. 141, No. 2, 04014090.

Kakrasul, J. I., Han, J., Rahmaninezhad, S. M., and Weldu, M., 2016, "Model Tests of Geosynthetic-Reinforced Earth Walls with Limited-Space Retained Fill," presented at the *Third Pan-American Conference on Geosynthetics*, Miami Beach, FL, North American Geosynthetics Society, Albany, NY, pp. 1279–1286.

Lajevardi, S. H., Dias, D., and Racinais, J., 2013, "Analysis of Soil-Welded Steel Mesh Reinforcement Interface Interaction by Pull-Out Tests," *Geotext. Geomembr.*, Vol. 40, pp. 48–57, https://doi.org/10.1016/j.geotexmem.2013.08.002

Lawson, W. D., Jayawickrama, P. W., Wood, T. A., and Surles, J. G., 2013, "Pullout Resistance Factors for Steel Reinforcements Used in TxDOT MSE Walls," presented at the *Geo-Congress; Stability and Performance of Slopes and Embankments III*, San Diego, CA, American Society of Civil Engineers, Reston, VA, pp. 44–53.

Leshchinsky, D. and Marcozzi, G. F., 1990, "Bearing Capacity of Shallow Foundations: Rigid Versus Flexible Models," *J. Geotech. Eng.*, Vol. 116, No. 11, pp. 1750–1756, https://doi.org/10.1061/(ASCE)0733-9410(1990)116:11(1750)

Madhav, M. R., Gurung, N., and Iwao, Y., 1998, "A Theoretical Model for the Pull-Out Response of Geosynthetic Reinforcement," *Geosynth. Int.*, Vol. 5, No. 4, pp. 399–424, https://doi.org/10.1680/gein.5.0128

Nayeri, A. and Fakharian, K., 2009, "Study on Pullout Behavior of Uniaxial HDPE Geogrids under Monotonic and Cyclic Loads," *Int. J. Civ. Eng.*, Vol. 7, No. 4, pp. 211–223.

Ochiai, H., Yasufuku, N., Yamaji, T., Xu, G. L., and Hirai, T., 1996, "Experimental Evaluation of Reinforcement in Geogrid-Soil Structure," presented at the *International Symposium on Earth Reinforcement*, Kyushu, Japan, A. A. Balkema, Rotterdam, the Netherlands, pp. 249–254.

Otani, J., Miyamoto, K., Mukunoki, T., and Hirai, T., 2001, "Visualization of Interaction Behavior between Soil and Reinforcement Using X-Ray CT," presented at the *International Symposium on Earth Reinforcement*, Fukuoka, Japan, Taylor & Francis US, Burlington, MA, Vol. 1, pp. 117–120.

Palmeira, E. M., 2004, "Bearing Force Mobilisation in Pull-Out Tests on Geogrids," *Geotext. Geomembr.*, Vol. 22, No. 6, pp. 481–509, https://doi.org/10.1016/j.geotexmem.2004.03.007

Palmeira, E. M., 2009, "Soil–Geosynthetic Interaction: Modelling and Analysis," *Geotext. Geomembr.*, Vol. 27, No. 5, pp. 368–390, https://doi.org/10.1016/j.geotexmem.2009.03.003

Patra, S. and Shahu, J. T., 2012, "Pasternak Model for Oblique Pullout of Inextensible Reinforcement," *J. Geotech. Geoenviron. Eng.*, Vol. 138, No. 12, pp. 1503–1513, https://doi.org/10.1061/(ASCE)GT.1943-5606.0000720

Perkins, S. W. and Cuelho, E. V., 1999, "Soil-Geosynthetic Interface Strength and Stiffness Relationships from Pullout Tests," *Geosynth. Int.*, Vol. 6, No. 5, pp. 321–346, https://doi.org/10.1680/gein.6.0156

Rahmaninezhad, S. M., Han, J., Weldu, M., and Kakrasul, J. I., 2016, "Effects of Methods of Applying Normal Stresses in Pullout Tests on Pressure Distributions and Pullout Resistance," presented at the *Third Pan-American Conference on Geosynthetics*, Miami Beach, FL, North American Geosynthetics Society, Albany, NY, pp. 1308–1315.

Rahmaninezhad, S. M., Yasrobi, S. S., and Eftekharzadeh, S. F., 2009, "Effects of Compaction in the Subgrade of the Reinforced Sand Backfills with Geotextile on Bearing Capacity," *Int. J. Civ. Eng.*, Vol. 12, pp. 320–328.

Roodi, G. H. and Zornberg, J. G., 2017, "Stiffness of Soil-Geosynthetic Composite under Small Displacements. II: Experimental Evaluation," *J. Geotech. Geoenviron. Eng.*, Vol. 143, No. 10, 04017076, https://doi.org/10.1061/(ASCE)GT.1943-5606.0001769

Sieira, A. C. C. F., Gerscovich, D. M., and Sayão, A. S. F. J., 2009, "Displacement and Load Transfer Mechanisms of Geogrids under Pullout Condition," *Geotext. Geomembr.*, Vol. 27, No. 4, pp. 241–253, https://doi.org/10.1016/j.geotexmem.2008.11.012

Sugimoto, M., Alagiyawanna, A. M. N., and Kadoguchi, K., 2001, "Influence of Rigid and Flexible Face on Geogrid Pullout Tests," *Geotext. Geomembr.*, Vol. 19, No. 5, pp. 257–277, https://doi.org/10.1016/S0266-1144(01)00011-5

Sukmak, K., Sukmak, P., Horpibulsuk, S., Han, J., Shen, S.-L., and Arulrajah, A., 2015, "Effect of Fine Content on the Pullout Resistance Mechanism of Bearing Reinforcement

Embedded in Cohesive-Frictional Soils," *Geotext. Geomembr.*, Vol. 43, No. 2, pp. 107–117, https://doi.org/10.1016/j.geotexmem.2014.11.010

Teixeira, S. H. C., Bueno, B. S., and Zornberg, J. G., 2007, "Pullout Resistance of Individual Longitudinal and Transverse Geogrid Ribs," *J. Geotech. Geoenviron. Eng.*, Vol. 133, No. 1, pp. 37–50, https://doi.org/10.1061/(ASCE)1090-0241(2007)133:1(37)

Tran, V. D. H., Meguid, M. A., and Chouinard, L. E., 2013, "A Finite–Discrete Element Framework for the 3D Modeling of Geogrid–Soil Interaction under Pullout Loading Conditions," *Geotext. Geomembr.*, Vol. 37, pp. 1–9, https://doi.org/10.1016/j.geotexmem.2013.01.003

Wang, Z., Jacobs, F., and Ziegler, M., 2016, "Experimental and DEM Investigation of Geogrid–Soil Interaction under Pullout Loads," *Geotext. Geomembr.*, Vol. 44, No. 3, pp. 230–246, https://doi.org/10.1016/j.geotexmem.2015.11.001

Weldu, M. T., Han, J., Rahmaninezhad, S. M., Parsons, R. L., and Kakrasul, J. I., 2015, "Pullout Resistance of Mechanically Stabilized Earth Wall Steel Strip Reinforcement in Uniform Aggregate," Report No. K-TRAN: KU-14-7, Kansas Department of Transportation, Topeka, KS, 57p.

Weldu, M. T., Han, J., Rahmaninezhad, S. M., Parsons, R. L., Kakrasul, J. I., and Jiang, Y., 2016, "Effect of Aggregate Uniformity on Pullout Resistance of Steel Strip Reinforcement," *J. Transp. Res. Board*, No. 2579, pp. 1–7, https://doi.org/10.3141/2579-01

Wilson-Fahmy, R. F., Koerner, R. M., and Sansone, L. J., 1994, "Experimental Behavior of Polymeric Geogrids in Pullout," *J. Geotech. Eng.*, Vol. 120, No. 4, pp. 661–677, https://doi.org/10.1061/(ASCE)0733-9410(1994)120:4(661)

Xiao, C., Han, J., and Zhang, Z., 2016, "Experimental Study on Performance of Geosynthetic-Reinforced Soil Model Walls on Rigid Foundations Subjected to Static Footing Loading," *Geotext. Geomembr.*, Vol. 44, No. 1, pp. 81–94, https://doi.org/10.1016/j.geotexmem.2015.06.001

Zornberg, J. G., Roodi, G. H., and Gupta, R., 2017, "Stiffness of Soil–Geosynthetic Composite under Small Displacements. I: Model Development," *J. Geotech. Geoenviron. Eng.*, Vol. 143, No. 10, pp. 04017075-1–13, https://doi.org/10.1061/(ASCE)GT.1943-5606.0001768